Electronic Supplementary Information (ESI)

Manipulating spin state to activate atomically dispersed Fe-N-C catalyst for oxygen reduction

Fan Liu,[a] Chengxiang Shi,[a] Lun Pan,[a] Zhen-Feng Huang,[*a] Xiangwen Zhang,[a] and Ji-Jun Zou[*a,b]

[a]Key Laboratory for Green Chemical Technology of the Ministry of Education, School of Chemical Engineering and Technology, Tianjin University, Tianjin 300072, China; Collaborative Innovative Center of Chemical Science and Engineering (Tianjin), Tianjin 300072, China; Zhejiang Institute of Tianjin University, Ningbo, Zhejiang, 315201, China.
[b]Qinghai Quality Certification Consulting and Inspection Center Co., Ltd., Qinghai, China.
E-mail: jj_zou@tju.edu.cn (J.-J. Zou) and zfhuang@tju.edu.cn (Z.-F. Huang).

1. Methods

1.1 Materials

$FeCl_2 \cdot 4H_2O$ (99%), 1,3,5-Benzenetricarboxylic acid (99%), melamine (99%), Nafion solution (~5 wt.%) were obtained from Sigma-Aldrich. Absolute ethanol and isopropanol were obtained from the Chemicals Testing and Calibration Laboratory. All chemicals were used as received. High-purity water (18.25 MΩ·cm) supplied by a Milli-Q Gradient A10 system was used in all of the experiments.

1.2 Electrochemical measurements

The number of electron transfer (n) during the reaction was mainly calculated by the Koutecky-Levich (K-L) equation:

$$J^{-1}=J_L^{-1}+J_K^{-1}=B^{-1}\omega^{-1/2}+J_K^{-1} \quad (1)$$

$$B=0.2nFC_0(D_0)^{2/3}\nu^{-1/6} \quad (2)$$

Where J and JK represent measured current density and diffusion-limited current density, respectively, n is the number of electron transfer during the ORR, F is Faraday constant (96485 C mol^{-1}), C_0 is the O_2 concentration in the electrolyte (C_0 =1.2×10^{-3} mol L^{-1}), D_0 is the O_2 diffusion coefficient ($D=1.9\times10^{-5}$), ν is the kinetic viscosity of the electrolyte (0.01 cm^2 s^{-1} for 0.1 M KOH) and ω indicates the electrode rotation rate.

The number of electron transfer (n) and the yield of H_2O_2 were calculated by the following two equations:

$$n = 4I_d\,(I_d+I_rN^{-1})^{-1} \quad (3)$$

$$H_2O_2\% = 200I_r\,(N\,I_d + I_r)^{-1} \quad (4)$$

Where I_d is the disk current, I_r is the ring current, and N (0.37) is the collection coefficient.

The durability tests were conducted by measuring the current vs. time (i-t) chronoamperometric response at potential 0.6 V for 80000s in O_2-saturated electrolyte. The tolerance to CH_3OH test was performed in chronoamperometric at 0.6 V in O_2-saturated 0.1 M KOH solution along with the injection of CH_3OH (3 M) at 1500s. All measured potentials in this work were converted with reference to the standard RHE, according to the Nernst equation of $E_{RHE} = E_{Ag/AgCl} + 0.21 + 0.059 \times pH$.

The turnover frequency (TOF) is estimated by the following Equation:

$$TOF=JS\,(4nF)^{-1} \quad (5)$$

Where, J (mA cm^{-2}) and S (0.196 cm^{-2}) represent the kinetic current density at 0.85 V and the surface area of glassy carbon disk, respectively, the number 4 means that 4 electrons are involved in reacting with per mole of O_2, F denotes Faraday·s constant (96485.3 C mol^{-1}), while n is the molecular weight of the corresponding atom calculated from the catalyst loading m.

The electrochemically active surface area (ECSA) was evaluated based on double layer capacitance (C_{dl}) in the non-Faradaic potential region. Specifically, the was tested via CV measurements at various scan rates (10, 20, 30, 40, 60, 80, and 100 mV s^{-1}). The Cdl was obtained by plotting (j_a-j_c) at 1.10 V vs. RHE (where j_a and j_c are the anodic and cathodic current densities, respectively) against the scan rates. The slope of the above profiles was twice of C_{dl}. The ECSA was calculated using the following equation:

$$ECSA=C_{dl}C_s^{-1} \quad (6)$$

Where C_s is the specific capacitance of a smooth surfance of materials under specific electrochemical condition. According to previous study, the value of was 0.04 m F cm^{-2} in this calculation.

Mass activity of the catalyst was estimated using the following equation:

$$I_{mass} = I_{kin} / M_{catalyst} \quad (7)$$

Specific activity expressed as the activity per real surface area, can be calculated as

$$I_{spec} = I_{kin} / A_{real} \quad (8)$$

In this equation, $M_{catalyst}$ denotes the absolute Fe loading (μg_{Fe}), A_{real} denotes the absolute electrochemically active surface area (m^2) and I_{kin} denotes the kinetic current (mA), which was calculated using: $I_{kin} = I_{0.8} \times I_{lim}/(I_{lim} - I_{0.8})$. $I_{0.8}$ and I_{kin} denote the geometric current at 0.8 V vs. RHE and the diffusion limited current, respectively.

The performance of Zn-air battery was measured in home-made electrochemical cells. The zinc-air battery was composed of a polished zinc foil as anode, 1×1cm^2 carbon paper loaded with catalysts as cathode and 6.0 M KOH with 0.2 M zinc acetate mixture aqueous solution served as the electrolyte. The catalyst loading of the 20 wt.% Pt/C or Fe_{SAC}-NC was 1 mg cm^{-2}.

1.3 DFT calculations

The ORR catalyze on FeN_4 and Fe_{SAC}-NC systems were calculated based on four-electron pathway.

$$O_2(g) + * \rightarrow O_2* \quad (9)$$

$$O_2* + H_2O(l) + e^- \rightarrow OOH* + OH^- \quad (10)$$

$$OOH* + e^- \rightarrow O* + OH^- \quad (11)$$

$$O* + H_2O(l) + e^- \rightarrow OH* + OH^- \quad (12)$$

$$OH* + e^- \rightarrow OH^- + * \quad (13)$$

In this case, * represents the active sites.

The adsorption energy of the *OOH, *O, and *OH intermediates was defined as the difference in energy between the adsorbed complex and the sum of the isolated Fe_{SAC}-NC catalyst and the isolated *OOH, *O, and *OH group.

The free energy (ΔG) is obtained by[1]

$$\Delta G = \Delta E + \Delta ZPE - T\Delta S + \Delta G_U + \Delta G_{pH} \quad (14)$$

where ΔE is the energy difference between the reactants and the products, which can be obtained directly by DFT calculation. ΔZPE and ΔS are the contributions to the free energy from the zero-point vibration energy and entropy, respectively. T is the temperature (298.15 K). $\Delta G_U = -eU$, here U is the potential applied to the electrode. ΔG_{pH} is the correction of the H^+ free energy.

The definition of the magnetic moment (M) is

$$M = N(\text{spin-up}) - N(\text{spin-down}) \quad (15)$$

$$M = M(3dxy) + M(3dx^2\text{-}y^2) + M(3dz^2) + M(3dxz) + M(3dyz) \quad (16)$$

Here, N(spin-up) and N(spin-down) denote the number of electrons in the spin-up and spin-down occupied states, respectively.[2,3] M (3*dxy*), M (3dx^2-y^2), M (3dz^2), M (3*dxz*), and M (3*dyz*) indicate the projected of magnetic moments on Fe 3*dxy*, 3dx^2-y^2, 3dz^2, 3*dxz*, and 3*dyz*, respectively.

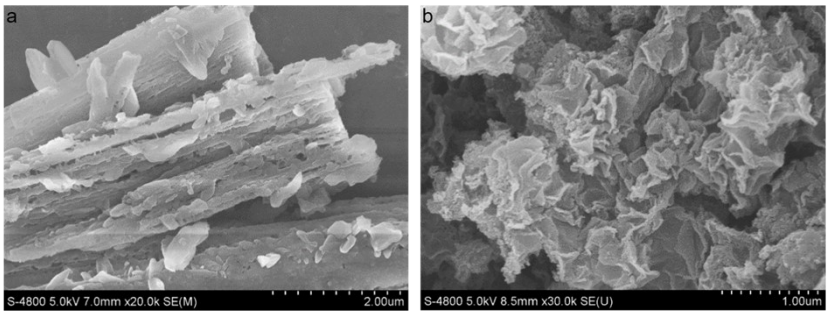

Figure S1. (a) SEM images of NC. (b) SEM images of Fe_{SAC}-NC.

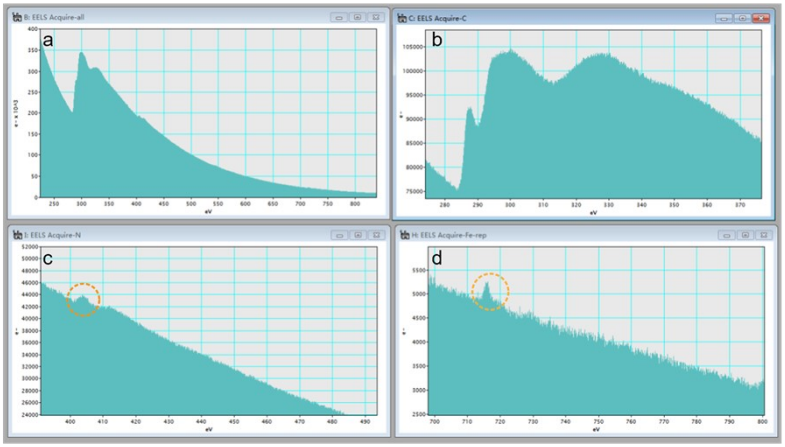

Figure S2. EELS point spectrum of Fe_{SAC}-NC. (a) full spectrum. (b) C spectrum. (c) N spectrum. (d) Fe spectrum.

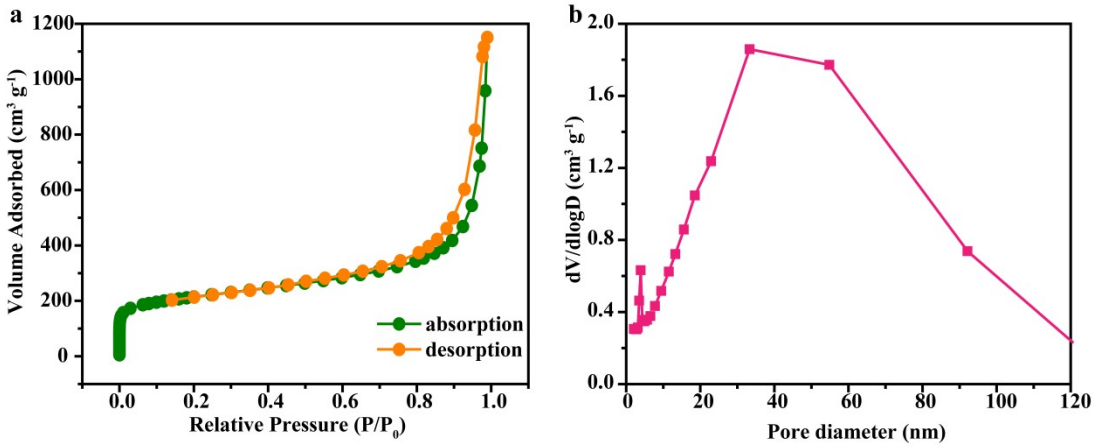

Figure S3. (a) N_2 adsorption-desorption curves of Fe_{SAC}-NC. (b) Pore distribution curve of Fe_{SAC}-NC.

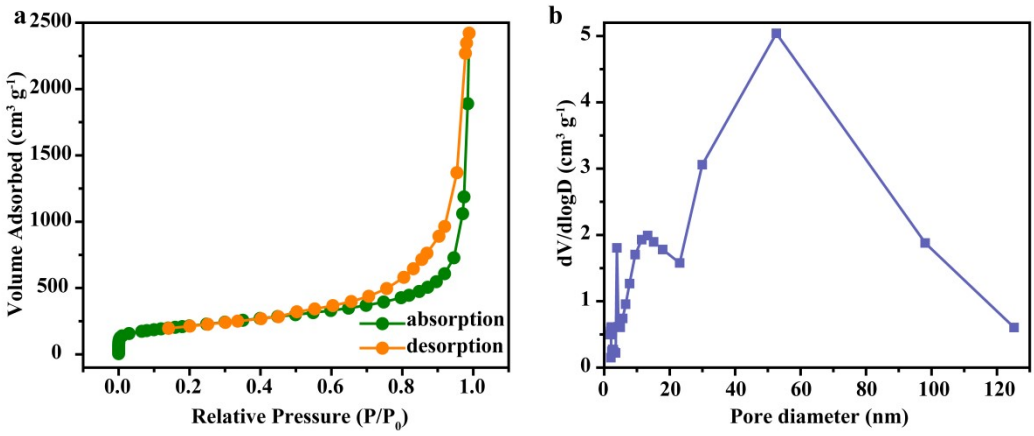

Figure S4. (a) N_2 adsorption-desorption curves of FeN_4. (b) Pore distribution curve of FeN_4.

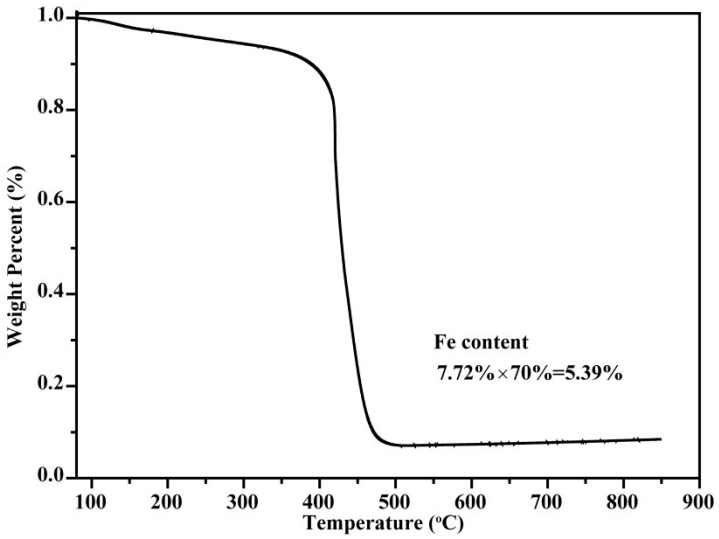

Figure S5. TGA curve of Fe_{SAC}-NC tested in air ambient.

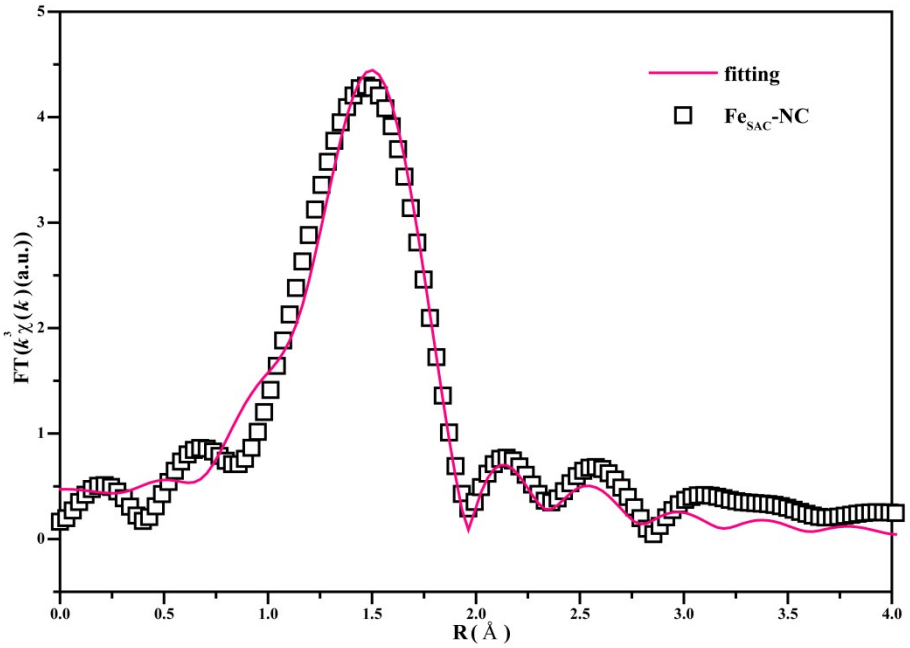

Figure S6. k^3-weighted Fourier transform spectra of Fe_{SAC}-NC and corresponding fitting curve.

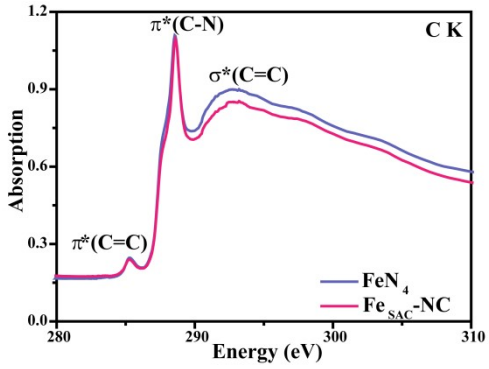

Figure S7. The normalized XANES spectra at the C K-edge of FeN_4 and Fe_{SAC}-NC.

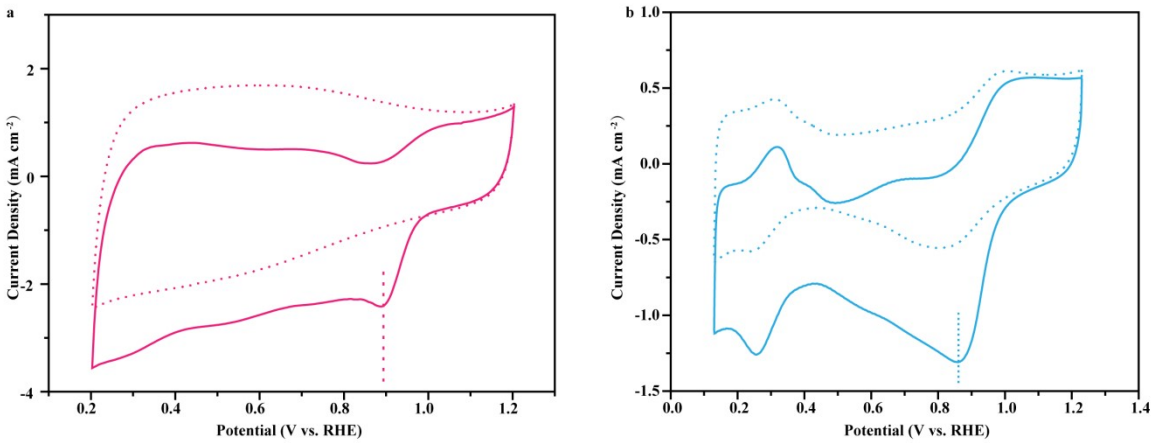

Figure S8. (a) The CV curves of Fe_{SAC}-NC in O_2 (solid) or Ar (dotted)-saturated 0.1M KOH. (b) The CV curves of 20% Pt/C in O_2 (solid) or Ar(dotted)-saturated 0.1M KOH.

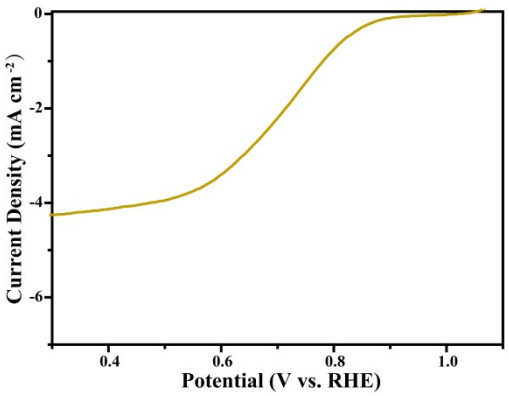

Figure S9. LSV curve of NC.

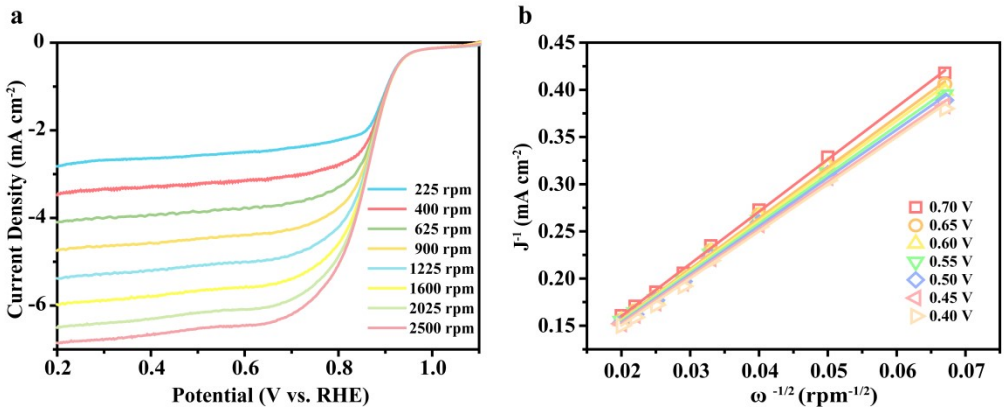

Figure S10. (a) LSVs curves of Fe_{SAC}-NC measured at different RDE rotating speed in O_2-saturated electrolytes. (b) The corresponding K-L plot of Fe_{SAC}-NC.

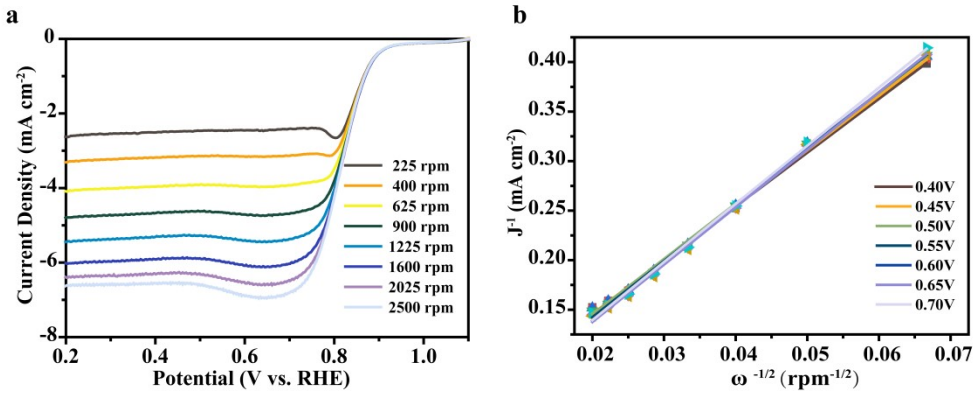

Figure S11. (a) LSVs curves of FeN_4 measured at different RDE rotating speed in O_2-saturated electrolytes. (b) The corresponding K-L plot of FeN_4.

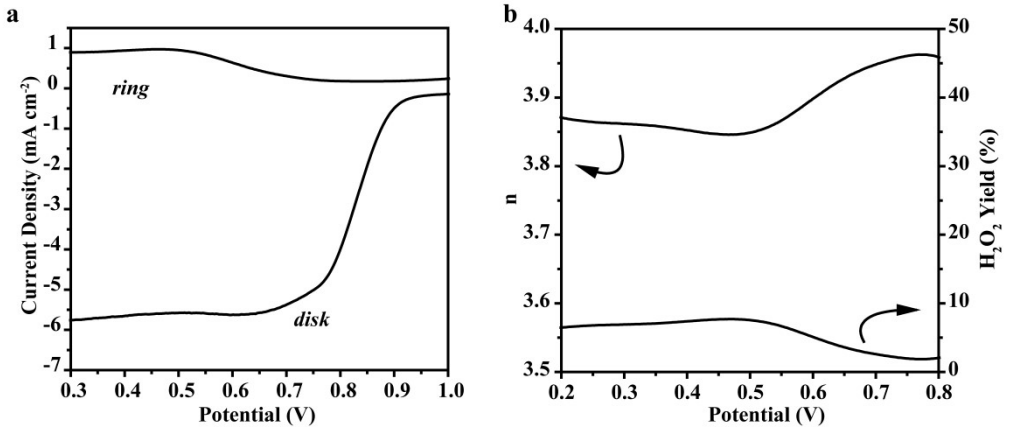

Figure S12. (a) RRDE test of FeN_4. (b) Electron transfer number (n) and H_2O_2 yield calculated from RRDE measurement of FeN_4.

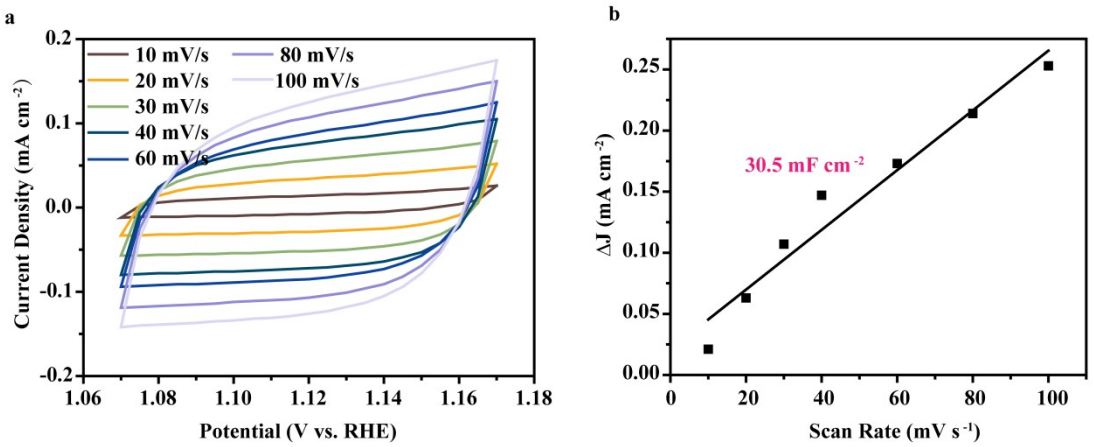

Figure S13. (a) CV curves for Fe_{SAC}-NC in the region of 1.06-1.18 V vs. RHE with various scan rates. (b) Scan-rate dependency of the current density for Fe_{SAC}-NC.

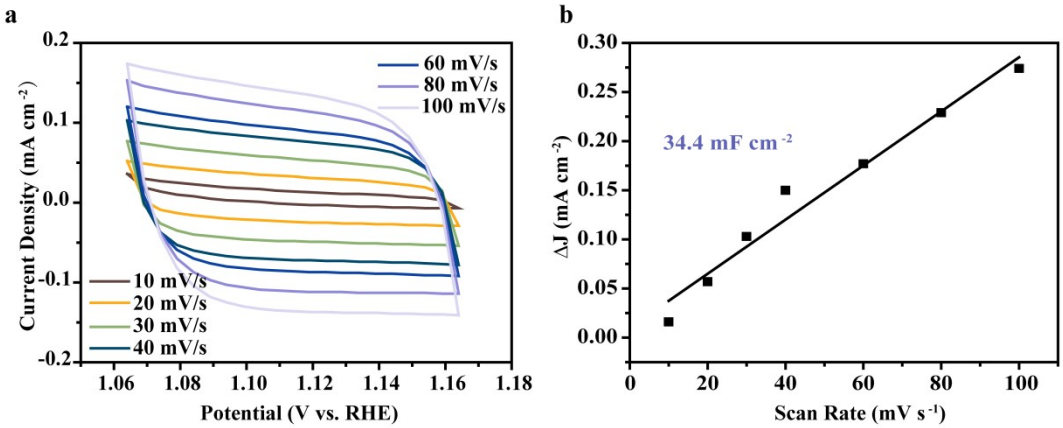

Figure S14. (a) CV curves for FeN_4 in the region of 1.06-1.18 V vs. RHE with various scan rates. (b) Scan-rate dependency of the current density for FeN_4.

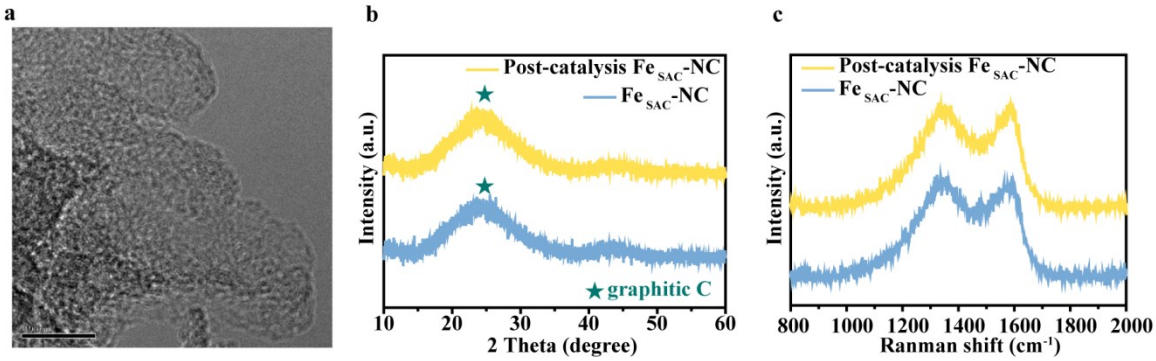

Figure S15. (a) HRTEM image of Fe_{SAC}-NC after ORR measurement. (b) XRD patterns of Fe_{SAC}-NC before and after ORR measurement. (c) Raman spectra of Fe_{SAC}-NC before and after ORR measurement.

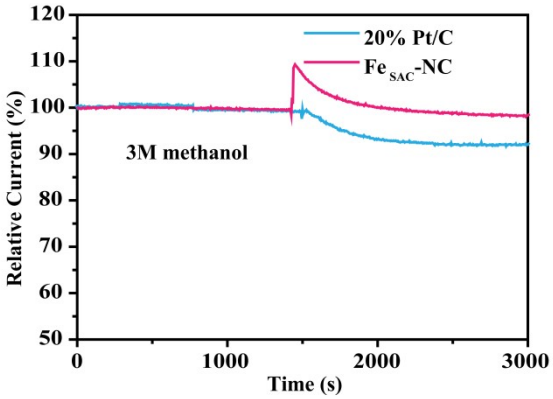

Figure S16. Methanol crossover effect test of Fe_{SAC}-NC and 20% Pt/C.

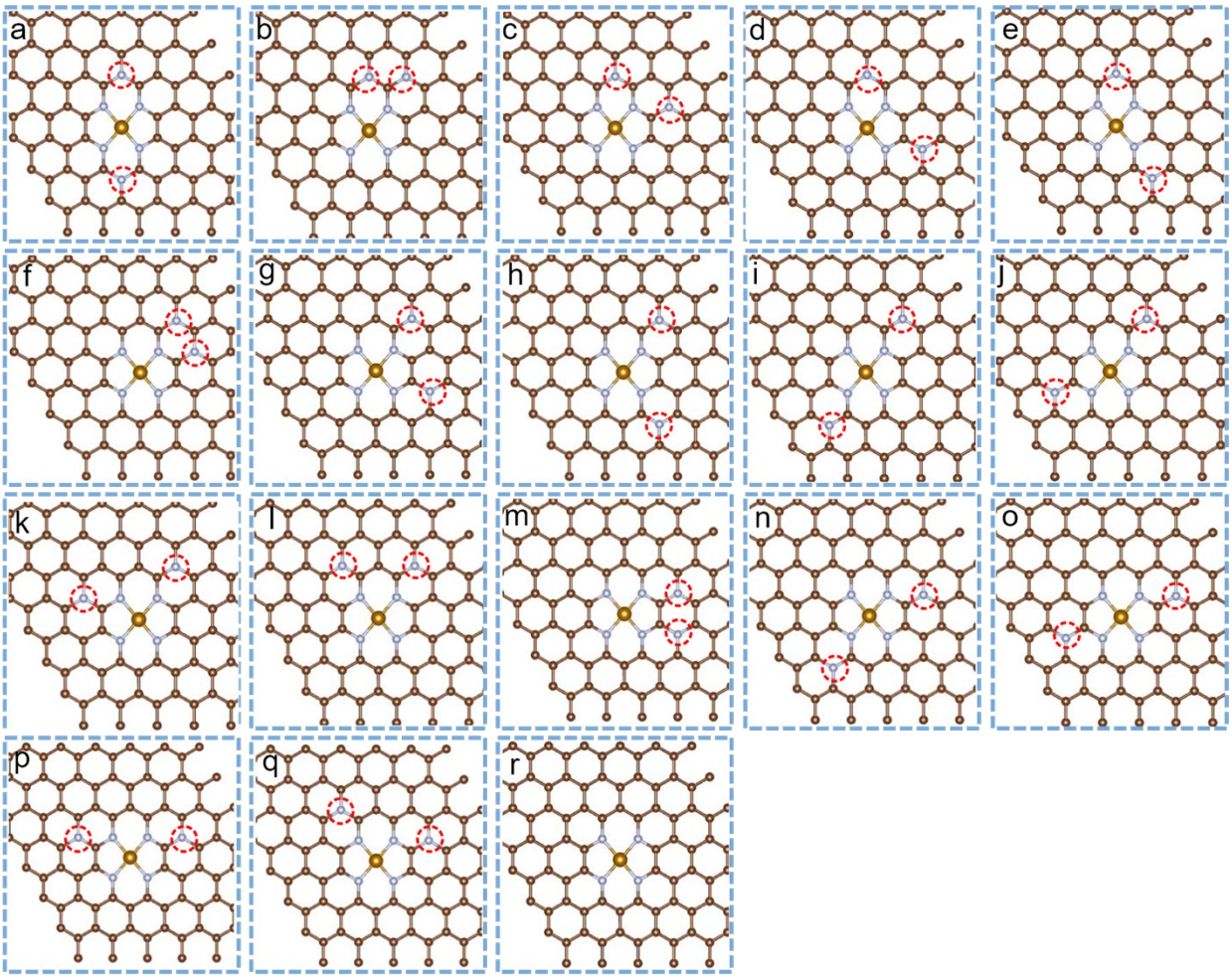

Figure S17. Optimized structure of (a) Fe_{SAC}-N_1C. (b) Fe_{SAC}-N_2C. (c) Fe_{SAC}-N_3C. (d) Fe_{SAC}-N_4C. (e) Fe_{SAC}-N_5C. (f) Fe_{SAC}-N_6C. (g) Fe_{SAC}-N_7C. (h) Fe_{SAC}-N_8C. (i) Fe_{SAC}-N_9C. (j) Fe_{SAC}-$N_{10}C$. (k) Fe_{SAC}-$N_{11}C$. (l) Fe_{SAC}-$N_{12}C$. (m) Fe_{SAC}-$N_{13}C$. (n) Fe_{SAC}-$N_{14}C$. (o) Fe_{SAC}-$N_{15}C$. (p) Fe_{SAC}-$N_{16}C$. (q) Fe_{SAC}-$N_{17}C$. (r) FeN_4. (The names are derived from the N atoms respective locations.)

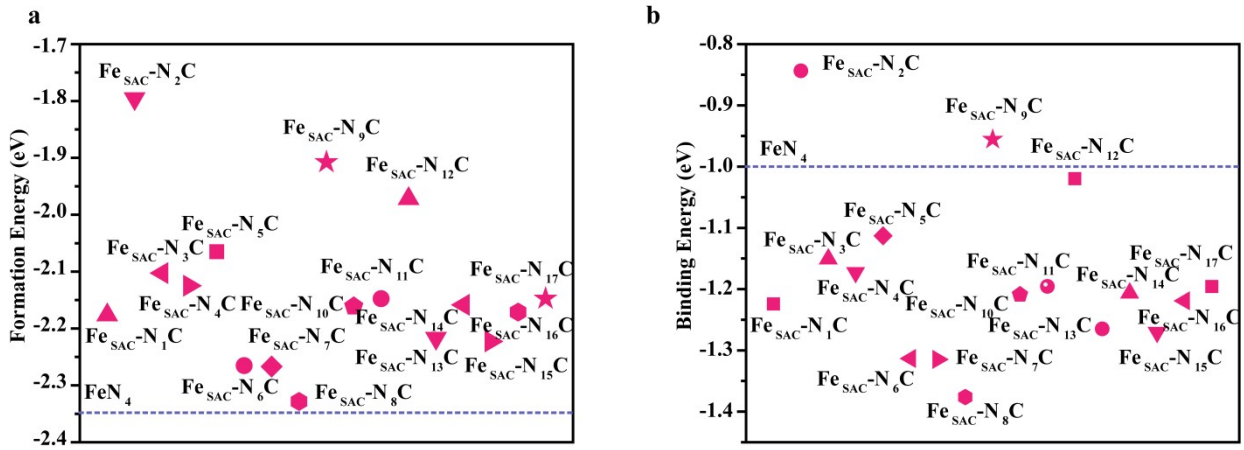

Figure S18. (a) The formation energy of Fe_{SAC}-N_XC (X=1-17). (b) The binding energy of Fe site on Fe_{SAC}-N_XC (X=1-17).

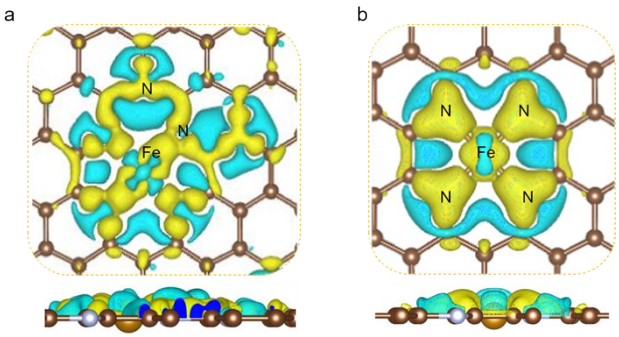

Figure S19. (a) Differential charge density of Fe_{SAC}-N_3C. (b) Differential charge density of FeN_4. Yellow regions indicate charge accumulation, while cyan regions indicate charge depletion. As for FeN_4, the electrons are transferred from Fe to N, resulting in a distinct depletion of charge density on the Fe site, which is consistent with the results of XAS and XPS.

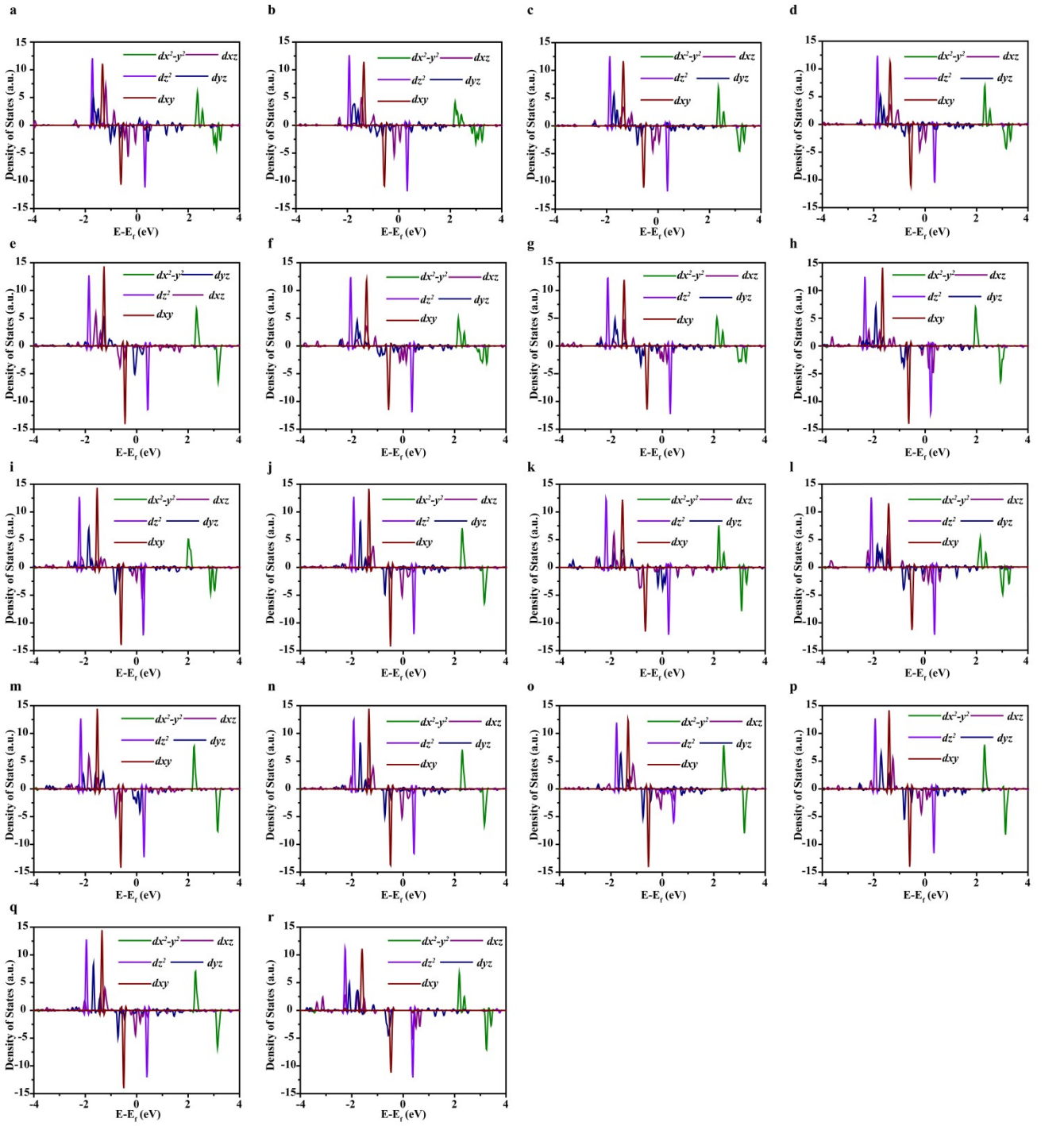

Figure S20. Detailed DOS of Fe d orbitals: (a) Fe_{SAC}-N_1C, (b) Fe_{SAC}-N_2C, (c) Fe_{SAC}-N_3C, (d) Fe_{SAC}-N_4C, (e) Fe_{SAC}-N_5C, (f) Fe_{SAC}-N_6C, (g) Fe_{SAC}-N_7C, (h) Fe_{SAC}-N_8C, (i) Fe_{SAC}-N_9C, (j) Fe_{SAC}-$N_{10}C$, (k) Fe_{SAC}-$N_{11}C$, (l) Fe_{SAC}-$N_{12}C$, (m) Fe_{SAC}-$N_{13}C$, (n) Fe_{SAC}-$N_{14}C$, (o) Fe_{SAC}-$N_{15}C$, (p) Fe_{SAC}-$N_{16}C$, (q) Fe_{SAC}-$N_{17}C$ and (r) FeN_4.

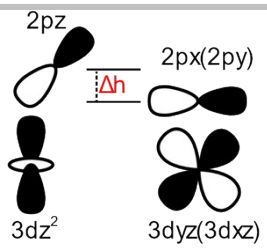

Figure S21. Schematic illustration of different hybridization modes of *3dyz (3dxz), 3dz²* and OH 2π* orbital. (Δh means the spatial height difference.)

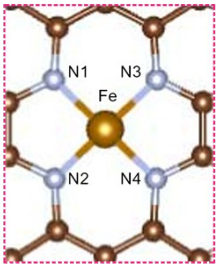

Figure S22. The schematic of each Fe-N bond length of Fe_{SAC}-N_xC(x=1-17).

Table S1. Summary of NC, Fe_{SAC}-NC, and FeN_4 BET data.

Sample	BET surface area ($m^2 \cdot g^{-1}$)	Total volume ($cm^3 \cdot g^{-1}$)	Mesopore size (nm)
NC	255	0.29	5.4
Fe_{SAC}-NC	725	1.66	15.4
FeN_4	752	3.77	21.2

Table S2. Elemental composition of Fe_{SAC}-NC.

elemental analyzer				ICP	TGA
C (wt.%)	N (wt.%)	O (wt.%)	H (wt.%)	Fe(wt.%)	
81.38	8.97	3.21	0.96	5.48	5.39

Table S3. EXAFS fitting parameters of Fe foil and Fe_{SAC}-NC.

Samples	Shell	N	R (Å)	$\Delta\sigma^2 \times 10^3$ (Å^2)	ΔE_0 (eV)	R-factor
Fe foil	Fe-Fe	8	2.42±0.01	6.8 ± 1.2	10.6 ± 0.8	0.037
	Fe-Fe	6	2.84±0.01	9.0 ± 2.1	10.1 ± 0.4	
FeN_4	Fe-N	4	1.89±0.01	3.1±1.6	1.2±0.1	0.019
Fe_{SAC}-NC	Fe-N	3.7	1.90±0.02	8.17± 1.1	-7.8±0.5	0.042

Table S4. Summarize the E_0 values of standard reference materials and Fe_{SAC}-NC.

Sample	Fe foil	Fe_2O_3	FeN_4	Fe_{SAC}-NC
E_0 (eV)	7112.216	7126.305	7122.311	7123.292

Table S5. Summary of the Mossbauer parameters and assignments to different Iron species in Fe_{SAC}-NC.

Fe species	IS (mm^{-1})	QS (mm^{-1})	LW (mm^{-1})	Content（%）	Valence-state
D1	-0.06	0.11	0.58	8.1	α-Fe
D2	0.33	1.38	0.53	30.2	FeN_4,LS
D3	-0.10	0.86	0.50	61.7	$Fe^{III}N_4$,MS

Table S6. Summarize the most near-term reported single atoms-based electrocatalysts.

Sample	Onset potential (V vs. RHE)	Half-wave potential (V vs. RHE)	Ref
Fe_{SAC}-NC	1.06	0.90	our work
Ru-SAS/SNC	0.998	0.861	[4]
Cu/Zn-NC	0.98	0.83	[2]
Co-N/C+NG	1.04	0.915	[3]
Fe-N-CDC/CNT	0.99	0.86	[4]
Fe-NiNC-50	1.0	0.84	[5]
FeSA/HNPC	0.92	0.83	[6]
Cu-S_1N_3	1.05	0.918	[7]
Ni-N_4/GHSs/Fe-N_4	0.93	0.83	[8]
Co_1-N_3PS/HC	1.00	0.91	[9]
PSTA-Co-1000	0.96	0.878	[10]
Fe-N/P-C-700	0.941	0.867	[11]
Fe/OES	1.00	0.85	[12]

Table S7. Fe-N1, Fe-N2, Fe-N3, Fe-N4 and the average Fe-N bond length over Fe-N-C catalysts.

Catalysts	Fe-N1 (Å)	Fe-N2 (Å)	Fe-N3 (Å)	Fe-N4 (Å)	Average Fe-N (Å)
Fe_{SAC}-N_1C	1.90	1.90	1.90	1.90	1.90
Fe_{SAC}-N_3C	1.91	1.90	1.91	1.89	1.90
Fe_{SAC}-N_4C	1.90	1.90	1.89	1.91	1.90
Fe_{SAC}-$N_{16}C$	1.92	1.89	1.92	1.89	1.91

Table S8. Adsorption free energies of *O, *OH, and *OOH on Fe_{SAC}-N_XC(X=1-17).

Catalysts	ΔG_{*O} (eV)	ΔG_{*OH} (eV)	ΔG_{*OOH} (eV)
Fe_{SAC}-N_1C	1.93	0.84	3.56
Fe_{SAC}-N_2C	1.74	0.86	3.54
Fe_{SAC}-N_3C	1.70	0.84	3.60
Fe_{SAC}-N_4C	1.81	0.86	3.51
Fe_{SAC}-N_5C	1.70	0.80	3.52
Fe_{SAC}-N_6C	1.66	0.86	3.48
Fe_{SAC}-N_7C	1.65	0.83	3.48
Fe_{SAC}-N_8C	1.65	0.85	3.49
Fe_{SAC}-N_9C	1.66	0.84	3.53
Fe_{SAC}-$N_{10}C$	1.66	0.82	3.53
Fe_{SAC}-$N_{11}C$	1.66	0.86	3.61
Fe_{SAC}-$N_{12}C$	1.75	0.82	3.49
Fe_{SAC}-$N_{13}C$	1.65	0.75	3.40
Fe_{SAC}-$N_{14}C$	1.65	0.83	3.49
Fe_{SAC}-$N_{15}C$	1.77	0.82	3.51
Fe_{SAC}-$N_{16}C$	1.76	0.85	3.53
Fe_{SAC}-$N_{17}C$	1.66	0.84	3.50
FeN_4	1.39	0.58	3.56

Table S9. Reaction free energy of elementary step for ORR at U = 0 V vs. RHE on Fe_{SAC}-N_XC(X=1-17).

Catalysts	ΔG_1 (eV)	ΔG_2 (eV)	ΔG_3 (eV)	ΔG_4 (eV)	ΔG_5 (eV)
Fe_{SAC}-N_1C	-0.51	-0.85	-1.63	-1.09	-0.84
Fe_{SAC}-N_2C	-0.52	-0.86	-1.80	-0.87	-0.86
Fe_{SAC}-N_3C	-0.55	-0.76	-1.90	-0.86	-0.84
Fe_{SAC}-N_4C	-0.55	-0.86	-1.82	-0.90	-0.80
Fe_{SAC}-N_5C	-0.52	-0.89	-1.70	-0.95	-0.86
Fe_{SAC}-N_6C	-0.70	-0.74	-1.82	-0.80	-0.86
Fe_{SAC}-N_7C	-0.50	-0.94	-1.83	-0.82	-0.83
Fe_{SAC}-N_8C	-0.42	-1.01	-1.84	-0.80	-0.85
Fe_{SAC}-N_9C	-0.46	-0.93	-1.87	-0.82	-0.84
Fe_{SAC}-$N_{10}C$	-0.51	-0.87	-1.88	-0.83	-0.82
Fe_{SAC}-$N_{11}C$	-0.71	-0.72	-1.85	-0.89	-0.86
Fe_{SAC}-$N_{12}C$	-0.67	-0.84	-1.82	-0.84	-0.82
Fe_{SAC}-$N_{13}C$	-0.54	-0.98	-1.75	-0.90	-0.75
Fe_{SAC}-$N_{14}C$	-0.53	-0.90	-1.84	-0.82	-0.83
Fe_{SAC}-$N_{15}C$	-0.53	-0.88	-1.74	-0.95	-0.82
Fe_{SAC}-$N_{16}C$	-0.53	-0.87	-1.77	-0.91	-0.85
Fe_{SAC}-$N_{17}C$	-0.53	-0.89	-1.84	-0.82	-0.84
FeN_4	-0.70	-0.67	-2.17	-0.81	-0.58

References

1. J. K. Norskov, J. Rossmeisl, A. Logadottir, L. Lindqvist, J. R. Kitchin, T. Bligaard and H. Jonsson, *J. Phys. Chem. B*, 2004, **108**, 17886-17892.
2. M. Tong, F. Sun, Y. Xie, Y. Wang, Y. Yang, C. Tian, L. Wang and H. Fu, *Angew. Chem. Int. Ed.*, 2021, **60**, 14005-14012.
3. X. Zhang, X. Xu, S. Yao, C. Hao, C. Pan, X. Xiang, Z. Q. Tian, P. K. Shen, Z. Shao and S. P. Jiang, *Small*, 2022, **18**, e2105329.
4. J. Lilloja, E. Kibena-Poldsepp, A. Sarapuu, J. C. Douglin, M. Kaarik, J. Kozlova, P. Paiste, A. Kikas, J. Aruvali, J. Leis, V. Sammelselg, D. R. Dekel and K. Tammeveski, *ACS Catal.*, 2021, **11**, 1920-1931.
5. X. Zhu, D. Zhang, C.-J. Chen, Q. Zhang, R.-S. Liu, Z. Xia, L. Dai, R. Amal and X. Lu, *Nano Energy*, 2020, **71**, 104597.
6. X. Jin, Y. Xie, J. Fu, C. Zhao, Y. Xu, Y. Lv, B. Zhang, K. Sun, R. Si and J. Huang, *ChemCatChem*, 2021, **13**, 2683-2690.
7. H. Shang, X. Zhou, J. Dong, A. Li, X. Zhao, Q. Liu, Y. Lin, J. Pei, Z. Li, Z. Jiang, D. Zhou, L. Zheng, Y. Wang, J. Zhou, Z. Yang, R. Cao, R. Sarangi, T. Sun, X. Yang, X. Zheng, W. Yan, Z. Zhuang, J. Li, W. Chen, D. Wang, J. Zhang and Y. Li, *Nat. Commun.*, 2020, **11**, 3049-3059.
8. J. Chen, H. Li, C. Fan, Q. Meng, Y. Tang, X. Qiu, G. Fu and T. Ma, *Adv. Mater.*, 2020, **32**, e2003134.
9. Y. Chen, R. Gao, S. Ji, H. Li, K. Tang, P. Jiang, H. Hu, Z. Zhang, H. Hao, Q. Qu, X. Liang, W. Chen, J. Dong, D. Wang and Y. Li, *Angew. Chem. Int. Ed.*, 2021, **60**, 3212-3221.
10. X. Wei, D. Zheng, M. Zhao, H. Chen, X. Fan, B. Gao, L. Gu, Y. Guo, J. Qin, J. Wei, Y. Zhao and G. Zhang, *Angew. Chem. Int. Ed.*, 2020, **59**, 14639-14646.
11. K. Yuan, D. Luetzenkirchen-Hecht, L. Li, L. Shuai, Y. Li, R. Cao, M. Qiu, X. Zhuang, M. K. H. Leung, Y. Chen and U. Scherf, *J. Am. Chem. Soc.*, 2020, **142**, 2404-2412.
12. C.-C. Hou, L. Zou, L. Sun, K. Zhang, Z. Liu, Y. Li, C. Li, R. Zou, J. Yu and Q. Xu, *Angew. Chem. Int. Ed.*, 2020, **59**, 7384-7389.